

MRI features as a helpful tool to predict the molecular subgroups of medulloblastoma: state of the art

Giovanna Stefania Colafati, Ioan Paul Voicu, Chiara Carducci, Evelina Miele, Andrea Carai, Simona Di Loreto, Antonio Marrazzo, Antonella Cacchione, Valerio Cecinati, Assunta Tornesello and Angela Mastronuzzi

Abstract: Medulloblastoma is the most common malignant pediatric brain tumor. Medulloblastoma should not be viewed as a single disease, but as a heterogeneous mixture of various subgroups with distinct characteristics. Based on genomic profiles, four distinct molecular subgroups are identified: Wingless (WNT), Sonic Hedgehog (SHH), Group 3 and Group 4. Each of these subgroups are associated with specific genetic aberrations, typical age of onset as well as survival prognosis. Magnetic resonance imaging (MRI) is performed for all patients with brain tumors, and has a key role in the diagnosis, surgical guidance and follow up of patients with medulloblastoma. Several studies indicate MRI as a promising tool for early detection of medulloblastoma subgroups. The early identification of the subgroup can influence the extent of surgical resection, radiotherapy and chemotherapy targeted treatments. In this article, we review the state of the art in MRI-facilitated medulloblastoma subgrouping, with a summary of the main MRI features in medulloblastoma and a brief discussion on molecular characterization of medulloblastoma subgroups. The main focus of the article is MRI features that correlate with medulloblastoma subtypes, as well as features suggestive of molecular subgroups. Finally, we briefly discuss the latest trends in MRI studies and latest developments in molecular characterization.

Keywords: childhood brain cancer, medulloblastoma, molecular characterization, molecular subgroups, MRI, pediatric brain tumors

Received: 30 October 2017; revised manuscript accepted: 28 February 2018.

Introduction

Medulloblastoma is the most common malignant pediatric brain tumor, accounting for about 15–20% of the central nervous system (CNS) malignancies, 40% of them being located in the posterior fossa.¹ Although survival rates have increased by 30% in the past 20 years, many patients still die from this disease.²

Histological features unveil a heterogeneous disease. Four variants of medulloblastoma have been identified: classic, desmoplastic/nodular (D/N), extensive nodularity (MBEN), anaplastic and large cell, the latter often coexisting in the large cell/anaplastic (LC/A) variant.^{3,4}

In recent years, an important advance in knowledge was starting to consider medulloblastoma not as a single disease, but as a heterogeneous mixture of various subgroups with distinct characteristics. Based on genomic profiles, four distinct molecular subgroups have been identified: Wingless (WNT), Sonic Hedgehog (SHH), Group 3 and Group 4.^{5,6} Each subgroup has shown specific survival, age demographics, and genetic aberrations.⁷ In WNT and SHH subgroups, the name results from the signal pathway involved that plays a prominent role in the pathogenesis of that subgroup.⁸ Molecular subgroups have shown correlation with clinical outcome. For this reason, molecular subgroups were integrated in the most recent version of WHO

Ther Adv Neurol Disord

2018, Vol. 11: 1–14

DOI: 10.1177/
1756286418775375

© The Author(s), 2018.

Reprints and permissions:
[http://www.sagepub.co.uk/
journalsPermissions.nav](http://www.sagepub.co.uk/journalsPermissions.nav)

Correspondence to:

Chiara Carducci
Department of Imaging,
Neuroradiology Unit,
Bambino Gesù Children's
Hospital, Piazza
Sant'Onofrio 4, 00165,
Rome, Italy.
chiara1.carducci@opbg.net

Giovanna Stefania Colafati
Department of Imaging,
Neuroradiology Unit,
Bambino Gesù Children's
Hospital, Rome, Italy

Ioan Paul Voicu
Department of Imaging,
Neuroradiology Unit
and Department of
Hematology/Oncology and
Stem Cell Transplantation,
Bambino Gesù Children's
Hospital, Rome, Italy

Evelina Miele
Antonio Marrazzo
Antonella Cacchione
Angela Mastronuzzi
Department of
Hematology/Oncology and
Stem Cell Transplantation,
Bambino Gesù Children's
Hospital, Rome, Italy

Andrea Carai
Department of
Neuroscience and
Neurorehabilitation,
Neurosurgery Unit,
Bambino Gesù Children's
Hospital, Rome, Italy

Simona Di Loreto
Dipartimento di Pediatria,
Università degli studi di
Chieti, Chieti, Italy

Valerio Cecinati
Pediatric Hematology and
Oncology Unit, Department
of Hematology,
Transfusion Medicine and
Biotechnology, Pescara,
Italy

Assunta Tornesello
Oncoematologia
Pediatria, Ospedale Vito
Fazzi, Lecce, Italy

classification of CNS malignancies⁴ and even in clinical practice. These medulloblastoma subgroups remain stable at recurrence and are likely remindful of original cells; the clinical outcome is known to vary among different subgroups.^{9–12}

Furthermore, recent research by Cavalli and colleagues on 763 medulloblastoma samples has unveiled the presence of intertumoral heterogeneity within the four medulloblastoma subgroups, thus delineating the presence of 12 subtypes based on gene expression and DNA methylation features, but the degree of heterogeneity and the extent of overlap is still unknown. This newfound heterogeneity within medulloblastoma subgroups could account for previously unexplained variation.¹³

Magnetic resonance imaging (MRI) has a key role in the diagnosis, surgical guidance and follow up of patients with medulloblastoma. MRI is performed for all patients with a brain tumor.¹⁴ An accurate and rapid subgroup prediction molecular method (nonenzymatic multiplexed assay) is already in use,¹⁵ but it could be helpful and less expensive to improve the potential information that can be deduced from a routine exam in these patients. Prior studies have shown that medulloblastomas may present with heterogeneous imaging aspects and that specific phenotypic radiologic features may reflect tumor histological and biological characteristics.^{16–19} These studies seem to indicate MRI as a promising tool for early detection of medulloblastoma subgroups.²⁰ In the future, the early identification of the subgroups could be helpful in the planning of surgical resection, radiotherapy and chemotherapy targeted treatments. Thompson and colleagues studied the prognostic value of the extent of resection in a subgroup-specific manner.²¹ In their results the benefit of increased extent of resection is largely attenuated after consideration of molecular subgroup.

The primary aim of this paper is to review the state of the art on MRI features shown to be helpful in predicting the molecular subgroups of medulloblastoma.

Molecular characterization of medulloblastoma subgroups

WNT is the least common molecular medulloblastoma subgroup and accounts for about 10–11% of all medulloblastomas.²² It shows a peak

incidence at 10–12 years of age, being very rare in infants, without gender predilection. Classic histology is most frequently encountered, with rare cases of the LC/A variant and metastatic dissemination.²³ The hallmark alteration in WNT tumors is the somatic activating mutations in exon 3 of β -catenin (CTNNB1), shown in 85% of WNT medulloblastoma and predictive of good outcome.²⁴ However, the biological effect of Wnt/ β -catenin signaling activation and the link with a better prognosis have not yet been fully clarified.²⁵ Monosomy 6 is the main recurrent structural chromosomal alteration (80–85%), usually found in an otherwise balanced genome. The next most common mutations are in DDX3X gene (with a possible role in β -catenin activation²⁶) and the missense mutations in TP53 (15% of cases), that, despite being a marker of high risk in the SHH subgroup, does not confer difference in survival for WNT patients.²⁷

Subgroup SHH represents 28–30% of all medulloblastomas, with a bimodal age distribution: it is more frequent in infants and adults, with a slight male predominance among infants.²⁸ These patients have an intermediate prognosis, with 5-year survival ranging between 60% and 80%, but the associated mutations in MYCN or TP53 oncogenes worsen the prognosis.²⁹ D/N and MBEN are characteristically associated with the SHH subtype (Figure 1); however, it is possible to observe classic or LC/A histology.²³ Typical genetic alterations lead to the over-activation of SHH signaling: the most common are the somatic or germline inactivating alterations or the loss of PTCH1 and SUFU, or the somatic missense mutations activating SMO.^{30,31} A few SHH patients present high-risk disease due to co-amplification of MYCN and GLI2, accompanied by inactivation of TP53.²⁷ Patients with Gorlin syndrome, carriers of a germline mutation on PTCH1, have a predisposition to develop basal-cell carcinoma and medulloblastoma, especially MBEN.³² An uncommon presentation of SHH subgroup medulloblastomas has also been reported in patients with rare diseases such as Fanconi anemia.³³

Group 3 accounts for about 25–28% of all medulloblastomas, but these patients have the worst survival and the highest rate of metastatic dissemination (Figure 2).^{9,34} More common in infants and younger children, Group 3 medulloblastomas are very rare in adults, with a male to female ratio of 2:1.²³ The principal histology is classic or LC/A

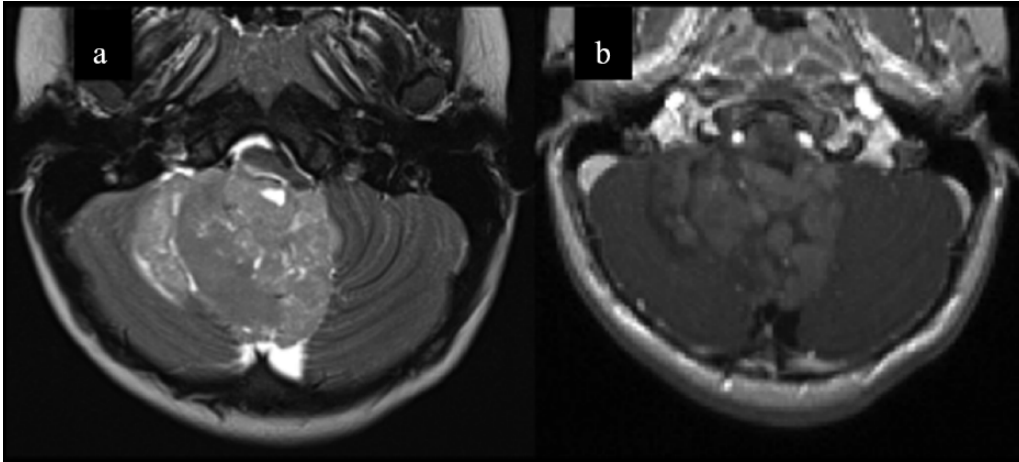


Figure 1. Example of SHH desmoplastic medulloblastoma. Two-year-old boy. Axial T2w(a) magnetic resonance images show an intraventricular mass in the fourth ventricle extending into the right Lushka foramen. Axial T1w postcontrast (b) images show associated heterogeneous contrast enhancement.

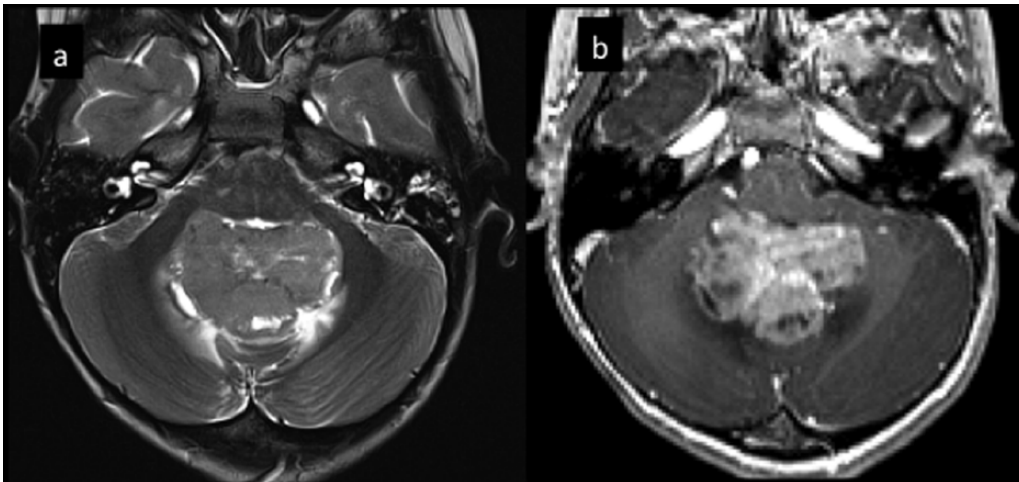


Figure 2. Example of Group 3 medulloblastoma. Five-year-old girl. Axial T2w(a) magnetic resonance images show an intraventricular mass in the fourth ventricle. Axial T1w postcontrast (b) image shows intense contrast enhancement and presence of cystic components.

and the tumor genome is considerably unbalanced, with a large number of broad alterations such as gain of chromosome 7 and iso-chromosome 17q. Associations with neurocutaneous syndromes such as tuberous sclerosis complex have also been described.³⁵ Group 4 medulloblastomas share many of these alterations (Figure 3).³⁶ The most common event is the MYC amplification (10–20%), followed by amplification of the OTX2 transcription factor, which accounts for 10% of patients and is mutually exclusive of MYC amplification.^{37–39}

Group 4 accounts for about 34–35% of medulloblastomas, making it the most common subgroup.²²

Rare in infants, they have a peak incidence in 10-year-old children, with a clear prevalence in males (sex ratio 3:1). They can have classic or LC/A histology.²³ Group 4 medulloblastomas have an intermediate prognosis and a high rate of metastasis and relapse: MYCN amplification, in contrast with the SHH subgroup, is not associated with the worst outcome.⁴⁰

MRI features

Medulloblastomas have a variable appearance on MRI. The tumor classically appears hyper- or isodense on computer tomography (Figure 4) and hypo- or isointense on T1- and T2-weighted MRI

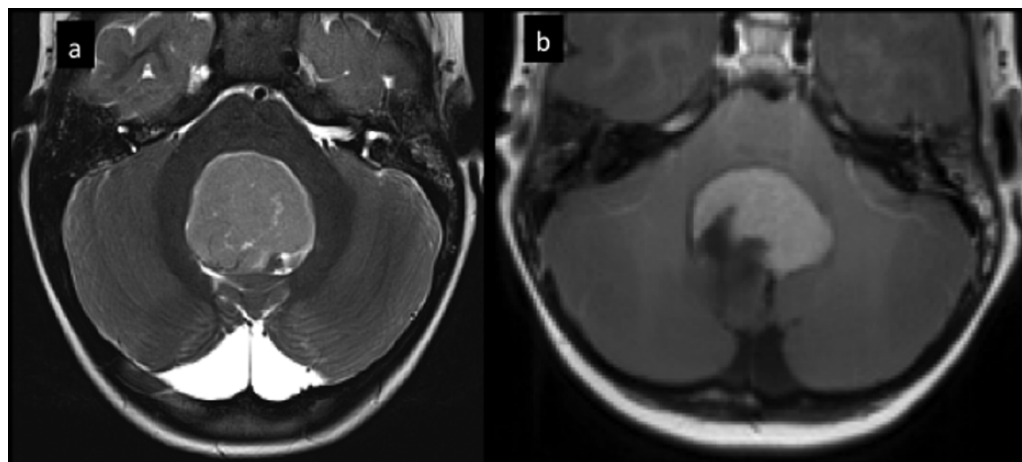


Figure 3. Example of desmoplastic Group 4 medulloblastoma. Four-year-old girl. Axial T2w(a) magnetic resonance images show an intraventricular mass in the fourth ventricle. Axial T1w postcontrast (b) images show associated homogeneous contrast enhancement.



Figure 4. Medulloblastoma in a 16-year-old boy. Axial computed tomography shows a hyperdense intraventricular mass with signs of mineralization (arrow).

based on differences in high cellularity/high nuclear-cytoplasmic ratio. They could appear homogeneous or heterogeneous due to intratumoral cyst or necrotic foci (about 50% of medulloblastomas¹⁷) and calcifications (10–20% of medulloblastomas). The features on contrast-enhanced images are also heterogeneous, with occasionally evidence of mild or no enhancement – up to 25% of cases in a recent report.^{19,20} An accurate analysis of these MRI features is necessary also in the differential diagnosis from others

brain tumors. Based on these findings, radiological assessment is difficult and it is strongly suggested that meticulous imaging guidelines at diagnosis and during follow up in patients with medulloblastomas (MBL) be followed (Table 1).^{41–42} Medulloblastomas are most commonly situated in the inferior vermis, and often compress the fourth ventricle, producing obstructive hydrocephalus, but hemispheric locations are also possible. Leptomeningeal dissemination across the cerebrospinal fluid (CSF) pathway can occur and is ordinarily situated at the Sylvian fissures, suprasellar subarachnoid space, posterior fossa cisterns or, rarely, cerebral hemispheric convexities. Thoracic and lumbosacral metastases are also relatively common.⁴³

Conventional MRI with morphological sequences is the first important step in the qualitative evaluation of tumor location and extension for medulloblastomas differential diagnosis with other tumor histotypes. Advanced MRI sequences, particularly diffusion-weighted imaging (DWI) with apparent diffusion coefficient (ADC) maps and spectroscopic studies improved information to achieve a quantitative analysis and have opened new opportunities to correlate imaging findings to medulloblastomas molecular subtypes.

DWI relies on microscopic water diffusion rate within tissues, which is inversely proportional to the cellularity of the tumor.

DWI and ADC maps have been used already for differential diagnosis of the major posterior fossa

Table 1. Brain and spine magnetic resonance imaging (MRI) protocol in our Institution for children with medulloblastoma at diagnosis and during follow up. Further recommendations are available from RAPNO (response assessment in pediatric neuro-oncology) guidelines for medulloblastoma and leptomeningeal seeding tumors.⁴²

Sequences	Slice thickness (mm)	
Brain MRI		
Axial T2 TSE	3	
Coronal T2 TSE Axial T2 FLAIR		
Axial DWI (b = 0,1000) with ADC	3	Consider additional DTI
3DT1 MPRAGE/SPACE	<1	Always perform if only MPRAGE is acquired Optional if SPACE is acquired
Axial T1 SE	3	
<i>After intravenous gadolinium contrast administration</i>		
3DT1 MPRAGE/SPACE + contrast	<1	Sagittal plane
Axial T1 TSE + contrast	3	Always perform if only MPRAGE is acquired Optional if SPACE is acquired
Axial T2 FLAIR + contrast	3	Optional
Spine MRI		
Sagittal T1 SE upper/lower + contrast	3	
Axial SE + contrast	3	
Sagittal T2 TSE	3	
Sagittal CISS/T2	<1	Optional
ADC, apparent diffusion coefficient; DTI, diffusion tensor imaging; DWI, diffusion-weighted imaging; FLAIR, fluid-attenuated inversion recovery; MPRAGE, radio-frequency pulses and rapid gradient-echo; SE, spin echo; SPACE, sampling perfection with application optimized contrasts using different flip angle evolution; TSE, turbo spin echo.		

tumors. High tumor cellularity of medulloblastoma classically results in restricted diffusion manifested by low ADC values (Figure 5).¹⁶ Differences in ADC values are still used to distinguish medulloblastomas from pilocytic astrocytomas (Figure 6).⁴⁴ Although the exact sensitivity of DWI in nonenhancing medulloblastomas needs to be established, its advantage over contrast-enhanced images has been previously reported. ADC value is typically lower than $800 \times 10^{-6} \text{ mm}^2/\text{s}$ because of the high cellularity of medulloblastomas.⁴⁴ Quantitative diffusion measurements could also be used to assess early treatment response, correlating to an increase in the ADC

value with a good treatment response, but clear data are not yet available in clinical practice.⁴⁵

Magnetic resonance spectroscopy (MRS) could provide useful information on tumor metabolism, and is already used to distinguish medulloblastomas from other posterior fossa tumors.^{46,47} Moreover, a significant metabolic heterogeneity within tumors of the same type has been observed, supposedly based on genetic profiles.^{48,49} Blüml and colleagues demonstrated, for the first time, that by *in vivo* analysis of tumor metabolites by MRS, using a five-metabolite model, it is possible to identify medulloblastoma

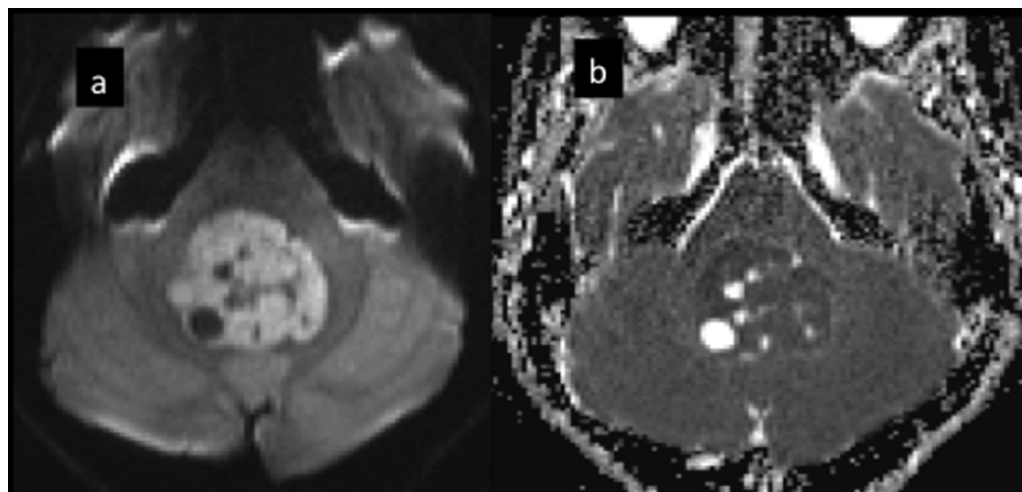


Figure 5. Diffusion-weighted images with $b=1000$ (a) and apparent diffusion coefficient maps (b) in a fourteen-year-old boy with histologically proven medulloblastoma. A posterior fossa intraventricular mass is seen. The lesion presents with diffusion restriction. Medulloblastomas typically present with diffusion restriction.

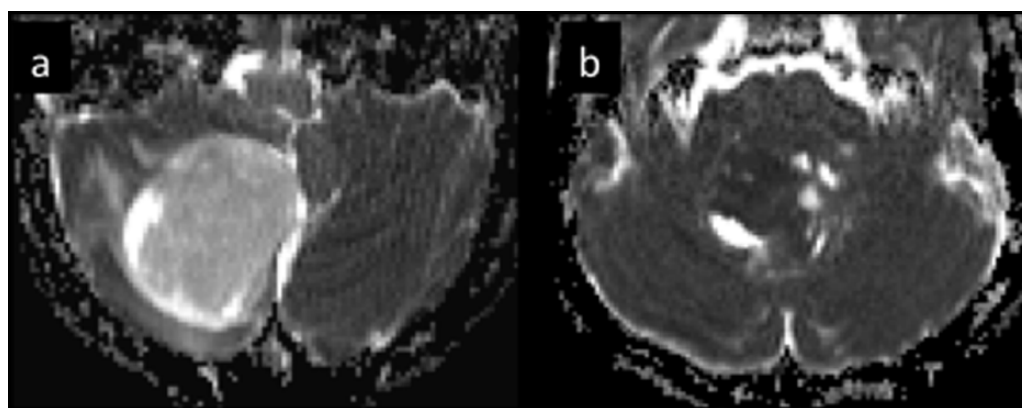


Figure 6. Apparent diffusion coefficient (ADC) maps in a six-year-old girl with pylocytic astrocytoma (a) and in a medulloblastoma (b, same patient as in Figure 4). In the patient with pylocytic astrocytoma the lesion does not show diffusion restriction. In the patient with medulloblastoma the lesion shows diffusion restriction.

molecular subgroups.⁵⁰ They described that Group 3 and Group 4 medulloblastomas had readily detectable taurine and creatine levels; SHH medulloblastomas also showed prominent choline and lipids peaks, notably low creatine levels, and little or no evidence of taurine. WNT medulloblastoma spectroscopic analysis was unreliable, given the small sample size described in this study.²³

MRI features suggestive for histologic medulloblastoma subtypes

Recent development in MRI evaluations can be used to differentiate histologically determined medulloblastoma subtypes.

Yeom and colleagues described how ADC values and other specific MRI features may distinguish medulloblastoma subtypes and aid in correct diagnosis and prognosis.¹⁴ In that study, the mean ADC ($\times 10^{-3} \text{ mm}^2/\text{s}$) ranged from 0.63 to 1.11, comparable to the reported mean ADC range reported in the literature.^{44,51,52} In addition, average minimum ADC value previously described was $0.49 \times 10^{-3} \text{ mm}^2/\text{s}$, similar to average minimum ADC values presented by Yeom and colleagues ($0.35 \times 10^{-3} \text{ mm}^2/\text{s}$).¹⁴ These variations in ADC value are justified by the presumably different selection techniques of region of interest (ROI). Some authors placed ROIs on only enhancing medulloblastoma sites, or in selected portions of tumors; conversely, Yeom and

colleagues manually drew the ROIs, defining total tumor boundaries to ensure reproducibility, and excluding hemorrhagic, cystic, or necrotic portions. The highest and lowest ADC values were observed in LC/A medulloblastomas and in classic medulloblastomas, respectively, confirming previous findings by Fruehwald-Pallamar and colleagues.^{14,52} ADC values are influenced by variations of water content in intra- and extracellular compartments. The highest cell density can be found in classic medulloblastomas. Small cells with scant cytoplasm characterize these tumors. Consequent relative water restriction might justify their relatively lower ADC values.^{53,54} In D/N medulloblastomas, ADC values are known to be lower (0.63×10^{-3} mm²/s), similarly to LC/A medulloblastomas. A reason for this behavior could be that extracellular water motion is restricted by dense reticulin fiber networks, which are typical of this subtype.^{14,55,56} Intratumoral cystic areas, necrosis and hemorrhage, excluded from ADC measurements, contribute to variations in cell density and could alter ADC values, as reported in adult glioblastoma multiforme studies.⁵⁷ The increasing metabolic demands of the cancerous tissue are referred to these data.¹⁴

‘Striking grapelike nodularity’ characterizes the computed tomography (CT) and MRI appearances of MBEN, with typically greater uptake on iodine-123 meta-iodo-benzyl-guanidine (MIBG) than the classic variant, revealed by single photon emission computed tomography (SPECT), probably due to neuronal differentiation of this variant.⁵⁸ An evident nodular aspect, well defined tumor mass and a particular macroscopic pattern, characterized by aggregate compact formation, that were organized in a ‘grapelike’ composition, were described. In addition, in some cases macrocysts were included in these structures. The mass appeared iso- or slightly hyperdense on CT, slightly hypointense on T1, hypointense on T2 and with noticeable contrast enhancement.⁵⁹ Contrast-enhanced MRI is useful to distinguish this tumor type from others and from pathologic processes in the cerebellum that are characterized by multinodular architecture, such as dysplastic gangliocytoma (Lhermitte–Duclos disease). Indeed, most nodular lesions of the cerebellum are not enhanced by MRI.⁴¹

The presence of ring enhancement is positively correlated with the LC/A subtype and with necrosis areas. From histological sections it has emerged

that the ring enhancement correlates with tumor necrosis areas. Currently, the presence of ring enhancement is more frequent in medulloblastoma with aggressive behavior, and it is not yet clear whether the cell necrosis is associated with abnormal tumor proliferation.¹⁴

MRI features suggestive of molecular medulloblastoma subgroups

Many studies have shown that medulloblastomas present heterogeneous imaging features, comprising site and enhancement characteristics.¹⁴ In this respect, an innovative finding is the identification of specific and peculiar radiological features that may reflect molecular medulloblastoma profiles. To date, few studies have focused on this approach.^{19,53}

At present, qualitative evaluation of the morphological sequences is deemed insufficient for characterization of molecular subtypes. Advanced MRI sequences have opened new opportunities to correlate imaging findings with molecular subtypes.

WNT

Perreault and colleagues published a study about the analysis of distinctive MRI features to predict medulloblastoma subgroups.²⁰ According to the authors’ model, tumor location was a key feature predictive of molecular subgroup. In their sample, WNT show a unique feature for this subgroup: the cerebellar peduncle/cerebellopontine angle cistern localization (75%).²⁰

A single study on 143 children affected by medulloblastoma focused on 16 WNT tumors (11.8%) in order to highlight specific WNT MRI features, correlated with its embryologic origin.⁶⁰ Specifically, WNT tumors seem to develop along an oblique-curved triangle centered on the foramen of Luschka, with one peak extending ventrolaterally to the CP-angle cistern, another postero-infero-medially to the cisterna magna, and the third postero-superomedially to the fourth ventricle (Figure 7). Previous studies observed that WNT tumors are located in the midline and always infiltrated the dorsal brain stem. The epicenter of the tumor had an important role in the evaluation, but tumor signal, cyst, necrosis and hemorrhage were also described through pre- and postoperative images. All WNT

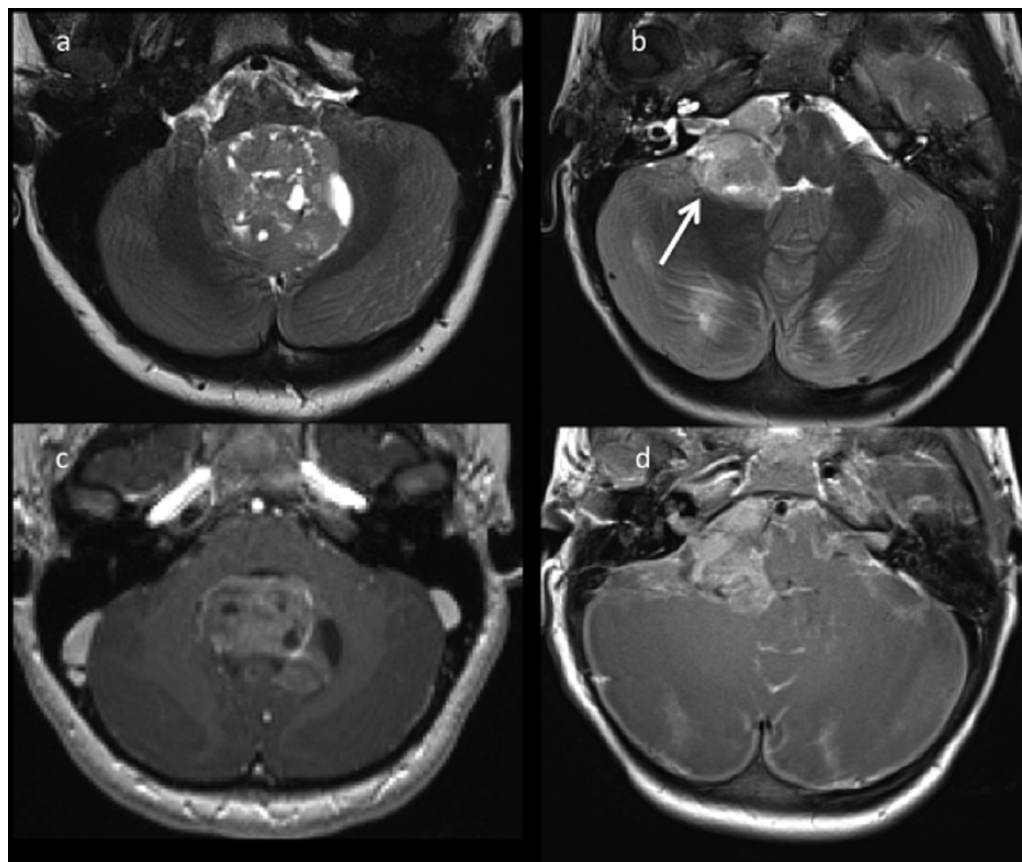


Figure 7. Magnetic resonance image of an eight-year-old girl (a,c) and of a three-year-old girl (b,d), both presenting with WNT medulloblastoma. Axial T2w (a,b) images of two patients show two masses localized respectively in the fourth ventricle (a) and in the right cerebellopontine angle (arrow) (b). Axial T1w postcontrast (c,d) images show heterogeneous enhancement of the two lesions.

tumors seemed mostly extra-parenchymal and attached to the surface of the brain stem and/or the cerebellum. The dentate nucleus, the superior and the middle cerebellar peduncle, the lateral brain stem, the infero-medial portion of the cerebellar hemisphere, and the floor of the fourth ventricle were some of the structures invaded. A laterality score was introduced to complete pre- and postoperative evaluation. The obtained results offered the hypothesis that WNT tumors are close to the midline but they are lateralized; the source areas are around the foramen of Luschka, superficial layers of the dorsolateral brain stem under the middle cerebellar peduncle and paramedian structures of the inferomedial cerebellar hemispheres. These results were in line with the new information on the origins and pathway involved.^{10,60,61} The laterality and the dominantly extra-parenchymal location of WNT tumors seemed to confirm that the lower rhombic lip could be the origin.

The relationship between the medulloblastoma and the brain stem was also evaluated: fewer than half (48%) of SHH tumors showed contact with the brain stem or an intraventricular expansion (19%). All other subgroups always had this contact. The key points were cuneate nucleus for WNT, and cuneate and cochlear nucleus for Group 3 and Group 4; almost all (87.5% WNT, 100% Group 3 and Group 4) showed infiltration of the fourth ventricle.²⁷

SHH

SHH has most commonly involved the cerebellar hemispheres (54%) in the analysis of Perreault and colleagues,²⁰ and the preferential localization of SHH medulloblastomas in the cerebellar hemispheres (Figure 8), following the higher frequency of D/N medulloblastomas involvement in this site, seems to be justified by SHH tumor

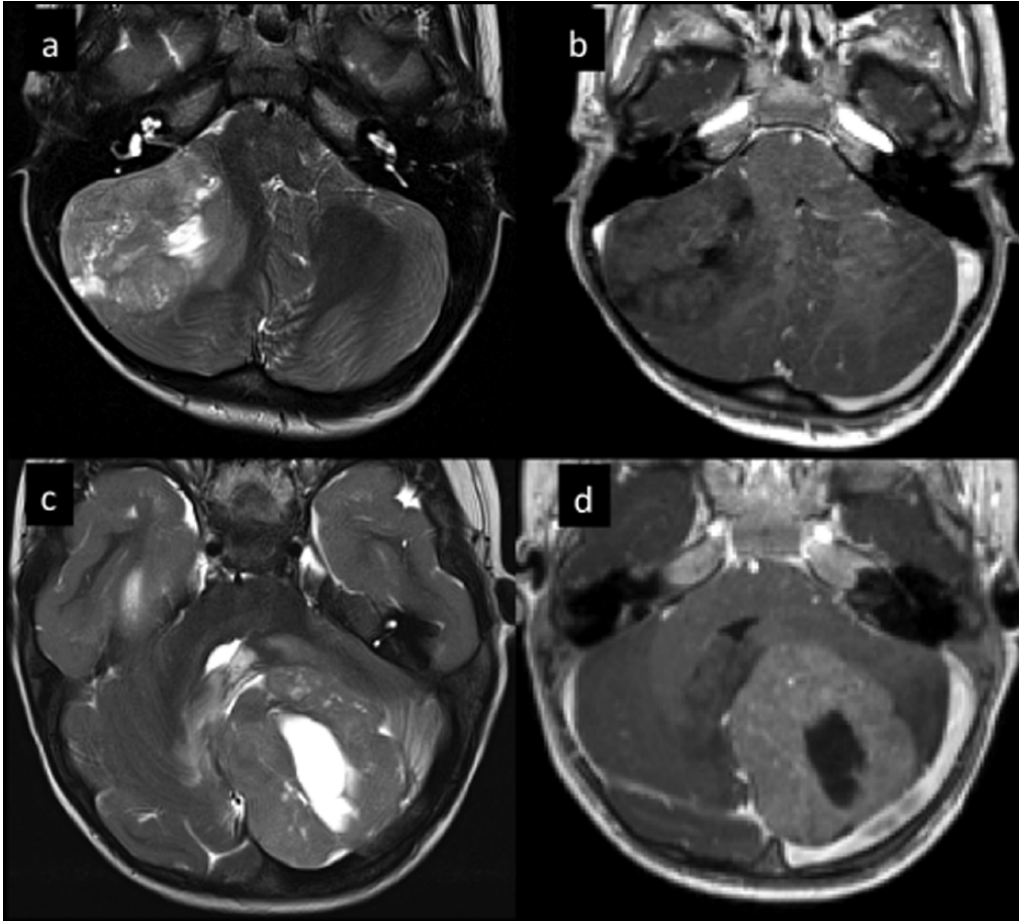


Figure 8. MRI of a six-year-old girl (a,c) and of a two-year-old girl (b,d) presenting with a classic and a desmoplastic SHH medulloblastoma. Axial T2w (a,c) images of two patients show two masses arising from the cerebellar hemispheres. Axial T1w postcontrast (c,d) images show almost no contrast enhancement of one lesion (c) and contrast enhancement in the other lesion (d).

origins,⁶⁰ while cochlear nucleus onset of SHH medulloblastomas in younger patients is not supported by a different SHH tumor location between infants and older patients.^{10,62}

A recent study analyzed a cohort of 71 patients with medulloblastoma to describe a correlation between molecular subgroups and location, broadening our understanding about the origins of molecular medulloblastoma subgroups.⁶³ An important observation was that all subgroups included some tumors that were only extracerebellar (37.5% WNT, 9.5% SHH, 13.3% Group 3, 22.2% Group 4), but only SHH medulloblastomas presented tumors that were only intracerebellar (52.4%). Hemispheric cerebellar tumor portions belonged mainly to the SHH subgroup.⁶³

As mentioned above, fewer than half (48%) of SHH tumors showed contact with the brain stem or an intraventricular expansion (19%). All other subgroups always had this contact: the key points were cuneate nucleus for WNT, and cuneate and cochlear nucleus for Group 3 and Group 4; almost all (87.5% WNT, 100% Group 3 and Group 4) showed infiltration of the fourth ventricle.²⁷ In line with previous studies, the predominant growth in the rostral cerebellar hemispheric region of SHH cancers led to the hypothesis that granule cells of this area may be more vulnerable to oncogenic alterations. This study also focused on the differences in various age groups in SHH type, describing a typical two-peak age distribution. Most SHH medulloblastomas occur in infants (≤ 3 years; 38.1%) or in young adults (≥ 16 years; 47.6%), while few SHH tumors develop in

children (>3 to <16 years; 14.3%), in line with data in the literature.³⁰ In addition, Wefers and colleagues describe two distinct SHH medulloblastoma age entities in which different locations between pediatric–adult and infant SHH medulloblastomas reflects the various gene expression profiles and, consequently, the distinct cell of origin.^{27,28,63} Many of the former (66.7% of child SHH and 80% of adult SHH) were only intracerebellar; conversely, 87.5% of infant SHH had an extracerebellar part and 25% were completely extracerebellar. In addition, adult and child SHH medulloblastomas frequently present a hemispheric growth, while infant ones show mostly a vermian development (62.5%). Exclusively rostral cerebellar localization was associated with adult and child SHH medulloblastomas, and not those in infants. The contact with the brain stem is mainly described for infant tumors (87.5%), while few adult (20%) and child (33.3%) SHH medulloblastomas have this. These data lead to the hypothesis that rostral and rostro-caudal hemispheric cerebellar localization is specific to child and adult SHH tumors; on the other hand, extracerebellar origins may be supposed for WNT, Group 3, Group 4 and infant SHH medulloblastomas.^{27,63}

Group 3 and Group 4

In order to describe a correlation between molecular subgroups and location, broadening our understanding about the origins of molecular medulloblastoma subgroups, it was reported 73% of Group 3 and 70% of Group 4 had a vermian localization.⁶³

In the evaluation of the relationship between medulloblastoma and brain stem, there is always a contact between them or an intraventricular expansion contact and an infiltration of the fourth ventricle. Cuneate and cochlear nucleus were contacted for Group 3 and Group 4.²⁷

Group 4 are characteristically nonenhancing tumors in the midline/fourth ventricle site: this is an important observation to distinguish Group 3 and Group 4.²⁰ The tumor margin was a useful predictor, but it was significantly limited by cohort studies and without homogeneity in MRI database analysis.²⁰

Establishing the nature of the boundary between Group 3 and Group 4 is of clinical importance as

outcomes differ, particularly in the setting of upfront metastatic dissemination.²¹

Finally, other advanced sequences could also be used to seek correlations with molecular medulloblastoma subgroups. A recent study explored the role of angiogenesis in order to identify clinically relevant biomarkers of tumor vascularity and survival in Group 3 medulloblastoma. The authors employed dynamic susceptibility weighted perfusion (DSC) and susceptibility weighted imaging (SWI) to scan with a 7 T magnet Group 3 xenografts implanted in nude rats.⁶⁴ Imaging metrics were correlated with vessel density and VEGFA rat protein expression. The authors found that VEGFA mRNA expression was significantly elevated in Group 3 medulloblastoma. In this cohort, VEGFA mRNA expression significantly influenced overall survival, with low VEGFA values being correlated with a survival advantage and high VEGFA values being correlated with a survival disadvantage. DSC MRI values were significantly correlated with vascularity and survival. SW MRI with ferumoxytol was a significant biomarker for survival. The authors concluded that DSC MRI and SWI were clinically relevant biomarkers for tumor vascularity and overall survival and could be used to direct the use of antivascular therapies for patients with Group 3 medulloblastoma.

Discussion

In this paper, we reviewed the state of the art on MRI features shown to be helpful in predicting the molecular subgroups of medulloblastoma. Most MRI researches on medulloblastoma subtypes with advanced sequences have employed DWI/ADC or spectroscopy, although other interesting approaches have been tested.⁶⁴

The latest trend in neuro-oncological studies is directed to the extraction of quantitative data from qualitative data, in order to identify possible MRI biomarkers. These should be precisely measurable and reproducible descriptors of the tumor.^{14,20} The combination of these features with genomic data could increase the diagnostic, prognostic and predictive yield of noninvasive radiological techniques, for the benefit of cancer patients, especially in children.

In this context, a promising field could be represented by ‘radiomic’ studies. ‘Radiomic’ studies are currently conducted to extract biomarkers

from advanced conventional sequences and to assign a quantitative value to MRI tumoral features, like dimensional, volumetric, morphological and localizing characteristics.^{65,66} Experimental research has confirmed that they can be currently useful to identify correlations but not to identify causes, so it is not currently expected that the only imaging assessment can replace histological and/or genetic data. Furthermore, radiologists should be aware that next-generation sequencing studies are still unveiling new findings on tumor pathways and genetic signatures on a frenetic pace.^{13,67,68} Where possible, MRI studies should confront and seek correlation with the latest histologic and molecular findings. The correlation between MRI and histological and molecular data could better target specific genomic research and possibly aid in the choice of precise biopsy site and surgical management, as well as providing potential support for histopathological data to guide the therapeutic approach.

MRI features of medulloblastoma could help neuro-oncologists, providing additional information with the goal of establishing accurate risk stratification at diagnosis.

The current standard of care dictates aggressive surgical approaches, aimed at total or near-total resection, given improved survival for patients in whom a gross total resection is achieved. However, a wider resection also carries significant risks of morbidity, including cerebellar mutism. A group of experts have recently analyzed the prognostic value of the extent of resection in a subgroup-specific manner in patients treated at centers participating in the Medulloblastoma Advanced Genomics International Consortium. The prognostic benefit of increased extent of resection for patients with medulloblastoma is attenuated after consideration of molecular subgroup. Maximum safe surgical resection is the standard of care, but in the case of small residual portions it is mandatory to consider the high likelihood of neurological morbidity, there is no definitive benefit to gross total resection compared with near-total resection.^{21,69,70} With further research and validation of MRI-based stratification, we envision the possibility of limiting biopsies for molecular profiling and neoadjuvant therapies. The limitations of these stratification methods are centered on access to the technology and skilled personnel to interpret the data, which are currently exclusive to some

specialist centers. The accuracy and feasibility of some MRI features for predicting molecular subgroups suggests that they may be a useful additional tool to the other strategies used for subgroup determination and treatment stratification in children with medulloblastoma.

Funding

This research received no specific grant from any funding agency in the public, commercial or not-for-profit sectors.

Conflict of interest statement

The authors declare that there is no conflict of interest.

References

1. Ostrom QT, Gittleman H, Fulop J, *et al.* CBTRUS statistical report: primary brain and central nervous system tumors diagnosed in the United States in 2008–2012. *Neuro Oncol* 2015; 17: 1–62.
2. Massimino M, Biassoni V, Gandola L, *et al.* Childhood medulloblastoma. *Crit Rev Oncol Hematol* 2016; 105: 35–51.
3. Louis DN, Ohgaki H, Wiestler OD, *et al.* The 2007 WHO classification of tumours of the central nervous system. *Acta Neuropathol* 2007; 114: 97–109.
4. Louis DN, Perry A, Reifenberger G, *et al.* The 2016 World Health Organization classification of tumors of the central nervous system: a summary. *Acta Neuropathol* 2016; 131: 803–820.
5. Taylor MD, Northcott PA, Korshunov A, *et al.* Molecular subgroups of medulloblastoma: the current consensus. *Acta Neuropathol* 2012; 123: 465–472.
6. Northcott PA, Korshunov A, Witt H, *et al.* Medulloblastoma comprises four distinct molecular variants. *J Clin Oncol* 2011; 29: 1408–1414.
7. Shih DJ, Northcott PA, Remke M, *et al.* Cytogenetic prognostication within medulloblastoma subgroups. *J Clin Oncol* 2014; 32: 886–896.
8. Ramaswamy V, Remke M, Bouffet E, *et al.* Recurrence patterns across medulloblastoma subgroups: an integrated clinical and molecular analysis. *Lancet Oncol* 2013; 14: 1200–1207.

9. Wang X, Dubuc AM, Ramaswamy V, *et al.* Medulloblastoma subgroups remain stable across primary and metastatic compartments. *Acta Neuropathol* 2015; 129: 449–457.
10. Gibson P, Tong Y, Robinson G, *et al.* Subtypes of medulloblastoma have distinct developmental origins. *Nature* 2010; 468: 1095–1099.
11. Gilbertson RJ and Ellison DW. The origins of medulloblastoma subtypes. *Annu Rev Pathol* 2008; 3: 341–365.
12. Cho YJ, Tsherniak A, Tamayo P, *et al.* Integrative genomic analysis of medulloblastoma identifies a molecular subgroup that drives poor clinical outcome. *J Clin Oncol* 2011; 29: 1424–1430.
13. Cavalli FMG, Remke M, Rampasek L, *et al.* Intertumoral heterogeneity within medulloblastoma subgroups. *Cancer Cell* 2017; 31: 737–754.
14. Yeom KW, Mobley BC, Lober RM, *et al.* Distinctive MRI features of pediatric medulloblastoma subtypes. *Am J Roentgenol* 2013; 200: 895–903.
15. Northcott PA, Shih DJ, Remke M, *et al.* Rapid, reliable, and reproducible molecular sub-grouping of clinical medulloblastoma samples. *Acta Neuropathol* 2012; 123: 615–626.
16. Brandão LA and Poussaint TY. Posterior fossa tumors. *Neuroimag Clin N Am* 2017; 27: 1–37.
17. Rasalkar DD, Chiu-wing Chu W, Paunipagar BK, *et al.* Paediatric intra-axial posterior fossa tumours: pictorial review. *Postgrad Med J* 2013; 89: 39–46.
18. Choudhri AF, Siddiqui A and Klimo P Jr. Pediatric cerebellar tumors: emerging imaging techniques and advances in understanding of genetic features. *Magn Reson Imaging Clin N Am* 2016; 24: 811–821.
19. Koeller KK and Rushing EJ. From the archives of the AFIP: medulloblastoma – a comprehensive review with radiologic-pathologic correlation. *Radiographics* 2003; 23: 1613–1637.
20. Perreault S, Ramaswamy V, Achrol AS, *et al.* MRI surrogates for molecular subgroups of medulloblastoma. *Am J Neuroradiol* 2014; 35: 1263–1269.
21. Thompson EM, Hielscher T, Bouffet E, *et al.* Prognostic value of medulloblastoma extent of resection after accounting for molecular subgroup: a retrospective integrated clinical and molecular analysis. *Lancet Oncol* 2016; 17: 484–495.
22. Ellison DW, Dalton J, Kocak M, *et al.* Medulloblastoma: clinicopathological correlates of SHH, WNT, and non-SHH/WNT molecular subgroups. *Acta Neuropathol* 2011; 121: 381–396.
23. Kool M, Korshunov A, Remke M, *et al.* Molecular subgroups of medulloblastoma: an international meta-analysis of transcriptome, genetic aberrations, and clinical data of WNT, SHH, Group 3, and Group 4 medulloblastomas. *Acta Neuropathol* 2012; 123: 473–484.
24. Ellison DW, Onilude OE, Lindsey JC, *et al.* Beta-catenin status predicts a favorable outcome in childhood medulloblastoma: the United Kingdom Children’s Cancer Study Group Brain Tumour Committee. *J Clin Oncol* 2005; 23: 7951–7957.
25. Di Giannatale A, Carai A, Cacchione A, *et al.* Anomalous vascularization in a Wnt medulloblastoma: a case report. *BMC Neurol* 2016; 16: 103.
26. Northcott PA, Jones DT and Kool M. Medulloblastomics: the end of the beginning. *Nat Rev Cancer* 2012; 12: 818–834.
27. Zhukova N, Ramaswamy V, Remke M, *et al.* Subgroup-specific prognostic implications of TP53 mutation in medulloblastoma. *J Clin Oncol* 2013; 31: 2927–2935.
28. Northcott PA, Hielscher T, Dubuc A, *et al.* Pediatric and adult sonic hedgehog medulloblastoma are clinically and molecularly distinct. *Acta Neuropathol* 2011; 122: 231–240.
29. Cho YJ, Tsherniak A, Tamayo P, *et al.* Integrative genomic analysis of medulloblastoma identifies a molecular subgroup that drives poor clinical outcome. *J Clin Oncol* 2011; 29: 1424–1430.
30. Kool M, Jones DT, Jäger N, *et al.* Genome sequencing of SHH medulloblastoma predicts genotype-related response to smoothed inhibition. *Cancer Cell* 2014; 25: 393–405.
31. Robinson G, Parker M, Kranenburg TA, *et al.* Novel mutations target distinct subgroups of medulloblastoma. *Nature* 2012; 488: 43–48.
32. Fujii K and Miyashita T. Gorlin syndrome (nevoid basal cell carcinoma syndrome): update and literature review. *Pediatr Int* 2014; 56: 667–674.
33. Miele E, Mastronuzzi A, Po A, *et al.* Characterization of medulloblastoma in Fanconi anemia: a novel mutation in the BRCA2 gene and SHH molecular subgroup. *Biomark Res* 2015; 3: 13.

34. Kawauchi D, Robinson G, Uziel T, *et al.* A mouse model of the most aggressive subgroup of human medulloblastoma. *Cancer Cell* 2012; 21: 168–180.
35. Moavero R, Folgiero V, Carai A, *et al.* Metastatic group 3 medulloblastoma in a patient with tuberous sclerosis complex: case description and molecular characterization of the tumor. *Pediatr Blood Cancer* 2016; 63: 719–722.
36. Jones DT, Jäger N, Kool M, *et al.* Dissecting the genomic complexity underlying medulloblastoma. *Nature* 2012; 488: 100–105.
37. Pei Y, Moore CE, Wang J, *et al.* An animal model of MYC-driven medulloblastoma. *Cancer Cell* 2012; 21: 155–167.
38. Bai RY, Staedtke V, Lidov HG, *et al.* OTX2 represses myogenic and neuronal differentiation in medulloblastoma cells. *Cancer Res* 2012; 72: 5988–6001.
39. Bunt J, Hasselt NA, Zwijnenburg DA, *et al.* OTX2 sustains a bivalent-like state of OTX2-bound promoters in medulloblastoma by maintaining their H3K27me3 levels. *Acta Neuropathol* 2013; 125: 385–394.
40. Shih DJ, Northcott PA, Remke M, *et al.* Cytogenetic prognostication within medulloblastoma subgroups. *J Clin Oncol* 2014; 32: 886–896.
41. Meyers SP, Kemp SS and Tarr RW. MR imaging features of medulloblastomas. *AJR Am J Roentgenol* 1992; 158: 859–865.
42. Warren KE, Vezina G, Poussaint TY, *et al.* Response assessment in medulloblastoma and leptomeningeal seeding tumors: recommendations from the Response Assessment in Pediatric Neuro-Oncology committee. *Neuro Oncol* 2018; 20: 13–23.
43. Zimmerman R. *Pediatric brain tumors*. 3rd ed. New York, NY: McGraw-Hill, 1992.
44. Rumboldt Z, Camacho DL, Lake D, *et al.* Apparent diffusion coefficients for differentiation of cerebellar tumors in children. *Am J Neuroradiol* 2006; 27: 1362–1369.
45. Erdem E, Zimmerman RA, Haselgrove JC, *et al.* Diffusion-weighted imaging and fluid attenuated inversion recovery imaging in the evaluation of primitive neuroectodermal tumors. *Neuroradiology* 2001; 43: 927–933.
46. Kovanlikaya A, Panigrahy A, Krieger MD, *et al.* Untreated pediatric primitive neuroectodermal tumor in vivo: quantitation of taurine with MR spectroscopy. *Radiology* 2005; 236: 1020–1025.
47. Panigrahy A, Krieger MD, Gonzalez-Gomez I, *et al.* Quantitative short echo time 1H-MR spectroscopy of untreated pediatric brain tumors: preoperative diagnosis and characterization. *Am J Neuroradiol* 2006; 27: 560–572.
48. Blüml S and Panigrahy A (eds). *MR spectroscopy of pediatric brain disorders*. New York, NY: Springer, 2013.
49. Yuneva MO, Fan TW, Allen TD, *et al.* The metabolic profile of tumors depends on both the responsible genetic lesion and tissue type. *Cell Metab* 2012; 15: 157–170.
50. Blüml S, Margol AS, Sposto R, *et al.* Molecular subgroups of medulloblastoma identification using noninvasive magnetic resonance spectroscopy. *Neuro Oncol* 2016; 18: 126–131.
51. Gauvain KM, McKinstry RC, Mukherjee P, *et al.* Evaluating pediatric brain tumor cellularity with diffusion-tensor imaging. *Am J Roentgenol* 2001; 177: 449–454.
52. Fruchwald-Pallamar J, Puchner SB, Rossi A, *et al.* Magnetic resonance imaging spectrum of medulloblastoma. *Neuroradiology* 2011; 53: 387–396.
53. Yamashita Y, Kumabe T, Higano S, *et al.* Minimum apparent diffusion coefficient is significantly correlated with cellularity in medulloblastomas. *Neurol Res* 2009; 31: 940–946.
54. Kono K, Inoue Y, Nakayama K, *et al.* The role of diffusion-weighted imaging in patients with brain tumors. *Am J Neuroradiol* 2001; 22: 1081–1088.
55. Liu H-Q, Yin X, Li Y, *et al.* MRI features in children with desmoplastic medulloblastoma. *J Clin Neurosci* 2012; 19: 281–285.
56. Pillai S, Singhal A, Byrne AT, *et al.* Diffusion-weighted imaging and pathological correlation in pediatric medulloblastomas: ‘they are not always restricted!’ *Childs Nerv Syst* 2011; 27: 1407–1411.
57. Lee EJ, terBrugge K, Mikulis D, *et al.* Diagnostic value of peritumoral minimum apparent diffusion coefficient for differentiation of glioblastoma multiforme from solitary metastatic lesions. *Am J Roentgenol* 2011; 196: 71–76.
58. Naitoh Y, Sasajima T, Kinouchi H, *et al.* Medulloblastoma with extensive nodularity: single photon emission CT study with iodine-123 metaiodobenzylguanidine. *Am J Neuroradiol* 2002; 23: 1564–1567.
59. Giangaspero F, Perilongo G, Fondelli MP, *et al.* Medulloblastoma with extensive nodularity: a variant with favorable prognosis. *J Neurosurg* 1999; 91: 971–977.

60. Patay Z, DeSain LA, Hwang SN, *et al.* Magnetic resonance imaging characteristics of WNT-subgroup pediatric medulloblastoma. *AJNR* 2015; 36: 2386–2393.
61. Teo WY, Shen J, Su JM, *et al.* Implications of tumor location on subtypes of medulloblastoma. *Pediatr Blood Cancer* 2013; 60: 1408–1410.
62. Grammel D, Warmuth-Metz M, von Bueren AO, *et al.* Sonic hedgehog-associated medulloblastoma arising from the cochlear nuclei of the brainstem. *Acta Neuropathol* 2012; 123: 601–614.
63. Wefers AK, Warmuth-Metz M, Pöschl J, *et al.* Subgroup-specific localization of human medulloblastoma based on pre-operative MRI. *Acta Neuropathol* 2014; 127: 931–933.
64. Thompson EM, Keir ST, Venkatraman T, *et al.* The role of angiogenesis in Group 3 medulloblastoma pathogenesis and survival. *Neuro Oncol* 2017; 19: 1217–1227.
65. Zhou M, Scott XJ, Chaudhury XB, *et al.* Radiomics in brain tumor: image assessment, quantitative feature descriptors, and machine-learning approaches. *Am J Neuroradiol* 2018; 39: 208–216.
66. Lambin P, Rios-Velazquez E, Leijenaar R, *et al.* Radiomics: extracting more information from medical images using advanced feature analysis. *Eur J Cancer* 2012; 48: 441–446.
67. Fu Zhao, Chunde Li, Qiangyi Zhou, *et al.* Distinctive localization and MRI features correlate of molecular subgroups in adult medulloblastoma. *J Neurooncol* 2017; 135: 353–360.
68. Northcott PA, Buchhalter I, Morrissy AS, *et al.* The whole-genome landscape of medulloblastoma subtypes. *Nature* 2017; 547: 311–317.
69. Robertson PL, Muraszko KM, Holmes EJ, *et al.* Incidence and severity of postoperative cerebellar mutism syndrome in children with medulloblastoma: a prospective study by the Children's Oncology Group. *J Neurosurg* 2006; 105(Suppl. 6): 444–451.
70. Beckwitt Turkel S, Krieger MD, O'Neil S, *et al.* Symptoms before and after posterior fossa surgery in pediatric patients. *Pediatr Neurosurg* 2012; 48: 21–25.

Visit SAGE journals online
[journals.sagepub.com/
home/tan](http://journals.sagepub.com/home/tan)

 SAGE journals